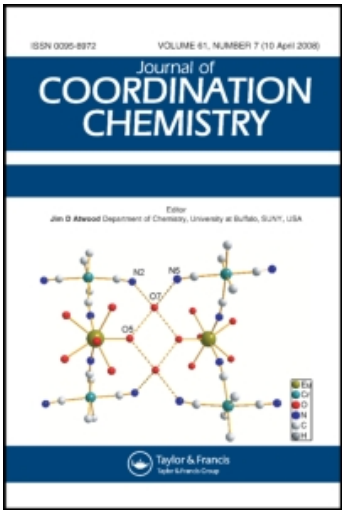

Journal of Coordination Chemistry
Publication details, including instructions for authors and subscription information:
http://www.informaworld.com/smpp/title~content=t713455674

DNA affinity and cleavage by naphthalene-based mononuclear and dinuclear copper(II) complexes

Jing Sun[ab]; Shu-Yi Deng[a]; Li Zhang[a]; Juan He[a]; Long Jiang[a]; Zong-Wan Mao[a]; Liang-Nian Ji[a]
[a] MOE Key Laboratory of Bioinorganic and Synthetic Chemistry, School of Chemistry and Chemical Engineering, Sun Yat-Sen University, Guangzhou 510275, China [b] School of Pharmaceutical Sciences, Guangdong Medical College, Dongguan 523808, China

To cite this Article Sun, Jing , Deng, Shu-Yi , Zhang, Li , He, Juan , Jiang, Long , Mao, Zong-Wan and Ji, Liang-Nian(2009) 'DNA affinity and cleavage by naphthalene-based mononuclear and dinuclear copper(II) complexes', Journal of Coordination Chemistry, 62: 20, 3284 — 3295
To link to this Article: DOI: 10.1080/00958970903055875
URL: http://dx.doi.org/10.1080/00958970903055875

Journal of Coordination Chemistry
Vol. 62, No. 20, 20 October 2009, 3284–3295

Taylor & Francis
Taylor & Francis Group

DNA affinity and cleavage by naphthalene-based mononuclear and dinuclear copper(II) complexes

JING SUN†‡, SHU-YI DENG†, LI ZHANG†, JUAN HE†, LONG JIANG†, ZONG-WAN MAO†* and LIANG-NIAN JI†

†MOE Key Laboratory of Bioinorganic and Synthetic Chemistry, School of Chemistry and Chemical Engineering, Sun Yat-Sen University, Guangzhou 510275, China
‡School of Pharmaceutical Sciences, Guangdong Medical College, Dongguan 523808, China

(*Received 21 November 2008; in final form 6 March 2009*)

Two copper(II) complexes with naphthalene ring $[Cu(L^1)(H_2O)](ClO_4)_2 \cdot H_2O$ (**1**) or $[Cu_2(L^2)(ClO_4)(H_2O)_3](ClO_4)_3 \cdot H_2O$ (**2**) (L^1 = 1-[bis(pyridine-2-ylmethyl)aminomethyl]naphthalene and L^2 = 1,4-di[bis(pyridine-2-ylmethyl)aminomethyl]naphthalene) were synthesized. Structural characterization of complex **2** by X-ray crystallography showed that the cations form a double-forficiform structure and each Cu(II) ion is bound by an in-plane N_3O_w-coordination. Thermal melting curves and fluorescence spectroscopes of complex-DNA binding indicate that both complexes can efficiently interact with calf thymus DNA and that the binding ability of complex **2** is greater than that of complex **1**. Viscosity measurements suggest that complex **2** partially intercalates between DNA base pairs via the naphthalene ring, whereas complex **1** most likely interacts with DNA through the electrostatic binding. In the presence of H_2O_2 and ascorbic acid, dinuclear complex **2** was more efficient than mononuclear complex **1** in cleaving double-stranded circular DNA into linear DNA. The interaction modes between the complexes and DNA were also discussed.

Keywords: Copper(II) complexes; Naphthalene; DNA interaction; DNA cleavage

1. Introduction

Metal ions have been shown to cause strand breakage in DNA, leading to cell death. There is growing evidence that endogenous substrates may induce DNA damage in the presence of metal ions, resulting in genomic instability and the induction of cancer. Thus, biomimetic DNA cleavage is of increasing importance in biotechnology and medicine. DNA cleavage activities of various biomimetic systems containing transitional metals and lanthanides have been extensively studied [1–11]. Recently, Cu(II) complexes, including mononuclear [12–25], dinuclear [26–35], trinuclear [36–40] and even macromolecular catalytic systems [41–43], have been used as catalysts for efficient cleavage of nucleic acids in the absence or presence of reducing agents. Mechanisms through which Cu(II) complexes degrade the nucleic acids involve hydrolytic cleavage and oxidative cleavage mediated by diffusible reactive oxygen species.

*Corresponding author. Email: cesmzw@mail.sysy.edu.cn

Journal of Coordination Chemistry
ISSN 0095-8972 print/ISSN 1029-0389 online © 2009 Taylor & Francis
DOI: 10.1080/00958970903055875

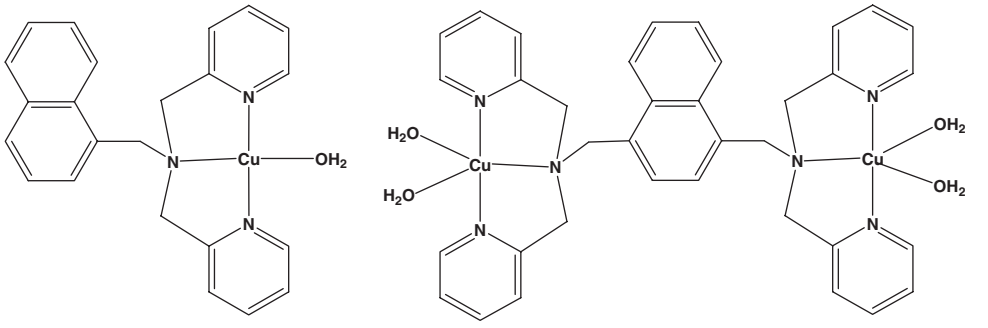

Scheme 1. Scheme view of complexes **1** and **2**.

Di-(2-picolyl)amine (dpa) is a well-defined ligand and has been used for the cleavage of bis(2,4-dinitrophenyl) phosphate [44]. The planar naphthalene ring of dpa can easily insert and stack between the base pairs of DNA duplex. In this study, to synthesize highly efficient DNA binding and cleavage agents, two dpa ligands were linked by 1,4-dimethylnaphthalene to generate a double-forficiform structure which can form a dinuclear Cu(II) complex with the central intercalator (scheme 1, complex **2**). At the same time, a dpa ligand was modified with monomethyl on the alpha-position of naphthalene to form a mononuclear Cu(II) complex (scheme 1, complex **1**) for comparison. Here, we report the synthesis, structures, DNA binding, and cleavage activities of the two newly synthesized Cu(II) complexes.

2. Experiment

2.1. *Materials*

Di-(2-picolyl)amine, 1-(chloromethyl)naphthalene, 2-(bromomethyl)naphthalene, 1,4-dimethylnaphthalene, and 1,5-dimethylnaphthalene were purchased from Sigma-Aldrich Chemical Co. Calf thymus DNA (CT DNA) and the pBR322 plasmid DNA were purchased from the Sino-American Biotechnology Company and BMI, respectively. Ethidium bromide (EB), 4-(2-hydroxyethyl)-1-piperazineethanesulfonic acid (HEPES), and tris(hydroxymethyl)-aminomethane (Tris) were purchased from AMRESCO Inc. Other reagents or analytical grade materials were obtained from commercial suppliers and used without further purification unless otherwise noted. Milli-Q water was used in all physical measurement experiments.

Caution: Although no problems were encountered in this work, transition-metal perchlorates are potentially explosive and should thus be prepared in small quantities and handled with care.

2.2. *Preparation of ligands and complexes*

2.2.1. $L^1 \cdot 2HClO_4 \cdot H_2O$. A tetrahydrofuran (THF) solution containing 1-chloromethylnaphthalene (0.354 g, 2 mmol) was added to a THF solution of dpa

(0.399 g, 2 mmol) at room temperature. Following the addition of triethylamine (0.202 g, 2 mmol), the mixture was heated under reflux for 5 h. After cooling, the triethylamine hydrochloride was filtered off and the filtrate was evaporated to obtain a syrup which was then dissolved in 4 mL of anhydrous methanol, and then perchloric acid was added into the solution dropwise under stirring to yield a white precipitate (0.764 g, 68.41%). Elemental Anal. Calcd (Found) for $C_{23}H_{21}N_3 \cdot 2HClO_4 \cdot H_2O$ (%): C, 49.54 (49.24); H, 4.52 (4.68); N, 7.54 (7.41). Electrospray ionization mass spectrometry (ESI-MS) (+ion) m/z Calcd (Found) for $[HL^1]^+$ 340.4 (340.3, 100%). ^{1}H NMR (d_6-dimethyl sufoxide (DMSO), 500 MHz): δ (ppm) 7.362–8.627 (m, 15H, ArH), 4.375 (s, 4H, NCH_2Py), 4.440 (s, 2H, NCH_2Ar).

2.2.2. 1,4-Dibromomethylnaphthalene. A mixture of 1,4-dimethylnaphthalene (1.18 g, 7.5 mmol) and N-bromosuccinimide (2.67 g, 15.0 mmol) in CCl_4 (75 mL) was refluxed for 30 min, and then benzoyl peroxide (15 mg) was added into the mixture. After another 2 h of reflux, the succinimide was filtered off and the solution was cooled to 0°C. The solid deposit was filtered and washed with MeOH to produce a white powder (0.986 g, 41.87%). Elemental Anal. Calcd (Found) for $C_{12}H_{10}Br_2$ (%): C, 46.17 (46.08); H, 3.23 (3.43); N, 0 (0.023).

2.2.3. $L^2 \cdot 4HClO_4 \cdot H_2O$. A THF solution containing 1,4-dibromomethylnaphthalene (0.314 g, 1 mmol) was added to a THF solution of dpa (0.399 g, 2 mmol) at room temperature. Following the addition of triethylamine (0.202 g, 2 mmol), the mixture was heated under reflux for 5 h. After cooling, the triethylamine hydrobromide was filtered off, the filtrate was evaporated, and the obtained syrup was dissolved in 4 mL of anhydrous methanol. Under stirring, perchloric acid was added dropwise into the solution to yield a white precipitate (0.672 g, 69.24%). Elemental Anal. Calcd (Found) for $C_{36}H_{34}N_6 \cdot 4HClO_4 \cdot H_2O$ (%): C, 44.62 (44.33); H, 4.16 (4.27); N, 8.68 (8.76). ESI-MS (+ion) m/z Calcd (Found) for $[HL^2]^+$ 551.3 (551.3, 100%); for $[HL^2(HClO_4)]^+$ 651.2 (651.1, 34%). ^{1}H NMR (D_2O, 500 MHz): δ (ppm) 7.319–8.281 (m, 22H, ArH), 4.075 (s, 8H, NCH_2Py), 4.318 (s, 4H, NCH_2Ar).

2.2.4. $[Cu(L^1)(H_2O)](ClO_4)_2 \cdot H_2O$ (1). The $L^1 \cdot 2HClO_4 \cdot H_2O$ (0.112 g, 0.2 mmol) was dissolved in 10 mL of water and 4 mL of aqueous solution of $Cu(ClO_4)_2 \cdot 6H_2O$ (0.089 g, 0.24 mmol) was added to the solution with stirring. Following the addition of NaOH (1.0 M) to obtain a pH of range 4–5, the solution was allowed to sit at room temperature for several days until green-blue powders were formed (0.073 g, 57.22%). Elemental Anal. Calcd (Found) for $[CuL^1(H_2O)](ClO_4)_2 \cdot H_2O$ (%): C, 43.31 (43.32); H, 3.95 (4.16); N, 6.59 (6.56). ESI-MS (+ion) m/z Calcd (Found) for $[(CuL^1)_2(ClO_4)(HClO_4)_3]^{3+}$ 402.3 (402.3, 100%); for $[(CuL^1)_2(ClO_4)_2(HClO_4)]^{2+}$ 551.1 (551.1, 47%). UV-Vis (H_2O): λ_{max} (ϵ) = 644 nm (82.9 $M^{-1}cm^{-1}$).

2.2.5. $[Cu_2(L^2)(ClO_4)(H_2O)_3](ClO_4)_3 \cdot H_2O$ (2). NaOH (1 M) was added to 10 mL of aqueous solution containing $Cu(ClO_4)_2 \cdot 6H_2O$ (0.081 g, 0.22 mmol) and $L^2 \cdot 4HClO_4 \cdot H_2O$ (0.097 g, 0.1 mmol) until pH reached 4–5, then the solution was allowed to sit at room temperature for several days to obtain the dark blue crystals (0.074 g, 64.48%) suitable for X-ray crystallographic analysis. Elemental Anal.

Calcd (Found) for $[Cu_2(L^2)(ClO_4)(H_2O)_3](ClO_4)_3 \cdot H_2O$ (%): C, 37.68 (37.70); H, 3.69 (3.70); N, 7.32 (7.37). ESI-MS (+ion) m/z Calcd (Found) for $[Cu_2(L^2)(ClO_4)(OH)]^{2+}$ 397.1 (397.2, 100%); for $[(Cu_2(L^2))_2(ClO_4)_5(OH)]^{2+}$ 934.9 (935.0, 57%); for $[Cu_2L^2(ClO_4)_2(OH)]^+$ 893.7 (893.0, 48%); for $[Cu_2(L^2)(ClO_4)_3]^+$ 976.1 (976.9, 35%). UV-Vis (H_2O): λ_{max} (ϵ) = 652 nm (127 $M^{-1}cm^{-1}$).

The ^1H NMR spectra and ESI-MS spectra of the ligands L^1 and L^2 are given in the "Supplementary material" (figures S1 and S2).

2.3. *General methods*

Elemental analysis (C, H, and N) was carried out with an Elementar Vario EL Elemental Analyzer. UV-Vis spectra were obtained from a Varian CARY 100 spectrophotometer and NMR spectra on a Varian INOVA NMR spectrometer with d_6-DMSO or D_2O as solvents for the ligands at room temperature (^1H at 500 MHz with wide-band proton decoupling). An LCQ DECA XP electrospray mass spectrometer was employed for the investigation of charged ligands in the mixture of water and methanol, and pH determinations were performed using a Metrohm 751 GPD Titrino pH meter. EB-stained agarose gels were imaged with Electrophoresis Documentation and Analysis System 120.

2.3.1. X-ray crystallography. Diffraction intensities for the complex **2** were collected at 293 K on a Siemens R3m diffractometer using the ω-scan technique. Lorentz-polarization and absorption corrections were applied. The structure was solved with direct methods using the SHELXS-97 software, and refined by full-matrix least-squares technique using SHELXL-97 software [45]. Anisotropic thermal parameters were applied to all non-hydrogen atoms. The organic hydrogen atoms were generated geometrically; the aqua hydrogen atoms were located from difference maps and refined with isotropic temperature factors. Analytical expressions of neutral-atom scattering factors were employed, and anomalous dispersion corrections were incorporated [46]. Crystal data and the details of data collection and refinement for complex **2** are summarized in table 1.

2.3.2. Thermal melting curves and ΔT_m calculation. The concentration of the CT DNA was determined by measuring the absorption intensity at 260 nm, with a known molar extinction coefficient value of 66.00 $M^{-1}cm^{-1}$ in Tris-HCl/NaCl buffer [20a, 47]. Thermal melting curves were obtained with a Cary 100 UV-Vis spectrophotometer connected to a temperature controller. The melting curves were recorded at different molar ratios of complex to DNA (r) by the absorption change at $\lambda = 260$ nm as a function of temperature ranging from 55°C to 95°C. T_m values were determined from the maximum of the first derivative or tangentially from the graph at the midpoint of the transition curves. ΔT_m values were calculated by subtracting the T_m value of the free nucleic acid from the T_m value of the nucleic acid with the complex.

2.3.3. Fluorescence spectroscopy of DNA-binding. The experiments were performed with 285 μM CT DNA solution in the absence or presence of the complexes at a concentration varying from 0 to 50 μM. In a typical binding experiment, CT DNA (285 μM) was added to EB (12.5 μM) containing Tris-HCl/NaCl buffer (pH 7.0) to

Table 1. Crystallographic data for complex **2**.

Complex	**2**
Empirical formula	$C_{72}H_{92}Cl_8Cu_4N_{12}O_{44}$
Formula weight	2367.34
Temperature (K)	293 (2)
Wavelength (Å)	0.71073
Crystal system	Monoclinic
Space group	*C2/c*
Unit cell dimensions (Å, °)	
a	39.365(9)
b	18.259(4)
c	28.308(7)
β	108.908(5)
Volume (Å^3), Z	19,250(8), 8
Calculated density (g cm^{-3})	1.634
Absorption coefficient (mm^{-1})	1.193
F(000)	9696
Crystal size (mm^3)	$0.12 \times 0.14 \times 0.39$
θ range for data collection (°)	1.52–26.00
Limiting indices	$-47 \le h \le 48$; $-22 \le k \le 22$; $-34 \le l \le 17$
Reflections collected	53,734
Independent reflection	18,836 [R(int) = 0.1178]
Goodness-of-fit on F^2	0.936
Final R indices [$I > 2\sigma(I)$]	$R_1 = 0.0735$, $wR_2 = 0.1739$
R indices(all data)	$R_1 = 0.2289$, $wR_2 = 0.2551$
Largest difference peak and hole (e A^{-3})	0.759, −0.447

$w = 1/[s^2F_o^2 + (0.0553P)^2 + 0.5928P]$, where $P = (F_o^2 + 2F_c^2)/3$.

achieve the maximum fluorescence intensity (excitation at 510 nm; emission at 601 nm). Aliquots of 1.0 mM stock solution of complex **1** or **2** in dimethylformamide (DMF) were added into the DNA/EB solution and the fluorescence was measured after each addition of the complex until a 50% reduction of the fluorescence intensity was observed. The fluorescence intensities were plotted against the complex concentration to obtain a slope, which provides a measure of the extent of binding of the complex to DNA.

2.3.4. Viscosity measurement of DNA-binding. Viscosity measurements were carried out using an Ubbelohde viscometer maintained at a constant temperature of 30.0 ± 0.1°C in a thermostatic bath. DNA samples with an average length of approximately 200 base pairs were prepared by sonication to minimize complexities arising from DNA flexibility [48]. Flow time was measured with a digital stopwatch. Each sample was measured three times and an average flow time was calculated. Data were presented as $(\eta/\eta^0)^{1/3}$ *versus* binding ratio ([Cu]/[DNA]) [49], where η is the viscosity of DNA in the presence of the complex and η^0 is the viscosity of DNA alone.

2.3.5. DNA cleavage. DNA cleavage rates of the two complexes at various catalyst concentrations were determined in 20 mM HEPES buffer (pH 8.1) at 37°C for different time intervals. Following the incubation of the pBR322 DNA and the complex for a defined time, 4 μL of loading buffer (0.05% bromophenol blue, 5% glycerol, and 2 mM ethylenediamine tetraacetic acid (EDTA)) was added to the reaction mixture and the samples were then electrophoresed on a 0.9% agarose gel at a constant voltage of 70 V

for 120 min and the gels were then imaged using the Electrophoresis Documentation and Analysis System 120. Densitometric analysis was performed using the analysis method in Image Tools 3.00. The intensities of the supercoiled pBR322 DNA were corrected by a factor of 1.42 because of its weaker staining by EB.

3. Results and discussion

3.1. *Crystal structure of complex 2*

As shown in Figure 1, complex **2** consists of a dinuclear $[Cu_2(L^2)(ClO_4)(H_2O)_3]^{3+}$ unit, three perchlorate anions, and a water of crystallization. The complex cation displayed a scorpion-like conformation with the naphthalene ring as its body and the Cu(II) units as its double-pincers. In the cation unit, Cu(1) is coordinated to three nitrogen atoms of the ligand and two oxygen atoms of water, forming a five-coordinated square pyramid geometry. Cu(2) is also five-coordinated with three nitrogen atoms of the ligand and an aqua oxygen atom forming a basal plane and the oxygen atom of perchlorate anion occupying the top of pyramid position. Adjacent coordinate units form a linear structure through the bridged perchlorate anion. Selected bond distances and angles of complex **2** are summarized in table 2.

3.2. *DNA affinities of the Cu(II) complexes*

The affinities of the two Cu(II) complexes to CT DNA were studied by measuring the changes in the melting temperature. Considerable increase in the melting temperature in each case was observed, demonstrating the stabilization of the double-stranded nucleic acids by the metal complexes. A markedly stronger stabilization effect of complex **2** over **1** was observed (table 3). In general, there are at least three interaction modes between metal complexes and DNA: electrostatic interaction, hydrophobic binding, and intercalating. The dinuclear complex **2** showed higher affinity to CT DNA than mononulear complex **1**, suggesting that the binding modes of complexes **1** and **2**

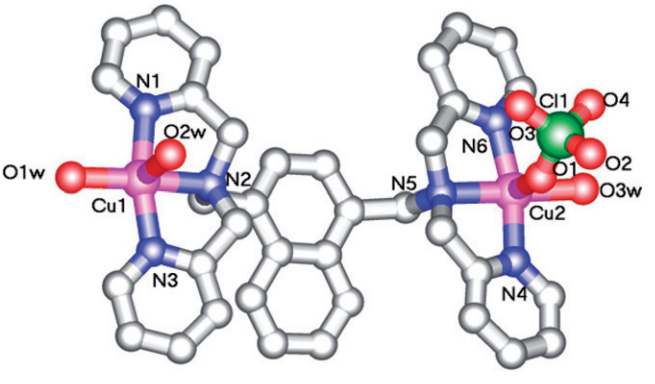

Figure 1. Crystal structure of complex **2**.

are different. A possible explanation for the high DNA affinity of complex **2** is that it may bind to the oxygen atoms of the phosphate backbone of DNA duplex [47].

The interactions of these Cu(II) complexes with CT DNA were characterized by a fluorescence spectrometry method. EB fluoresces when bound to DNA and a competitive binding of the complex to DNA causes the displacement of EB, leading to a reduction in the emission intensity. An obvious decrease of the emission intensity was observed upon the addition of the title complexes to the DNA/EB solutions (figure 2), indicating that the intercalation of the complexes was accompanied by their replacement of the EB molecules bound to DNA. Moreover, complex **2** showed greater reduction in the emission intensity than complex **1** at the same concentration, suggesting that complex **2** has a higher DNA-binding affinity than complex **1**. This finding was consistent with the results obtained from the melting temperature experiments.

Viscosity measurements are sensitive to changes of DNA length, and thus are regarded as the least ambiguous and the most critical tests for the binding mode of DNA to the metal complex in a solution [50–52]. A classical intercalation of the metal complex between DNA base pairs increases the length of the DNA helix due to the separation of base pairs to accommodate the bound ligand, leading to the increase of DNA viscosity. In contrast, a semi-intercalation of ligand could bend (or kink) the DNA helix, thus reducing its effective length and accordingly its viscosity.

Table 2. Selected bound lengths (Å) and angles (°) for complex **2**.

Cu(1)–O(1W)	1.949(6)	Cu(1)–O(2W)	2.336(6)
Cu(1)–N(1)	2.001(7)	Cu(1)–N(2)	2.012(6)
Cu(1)–N(3)	1.960(8)	Cu(2)–O(1)	2.485(6)
Cu(2)–O(3W)	1.966(6)	Cu(2)–N(4)	1.969(7)
Cu(2)–N(5)	2.021(7)	Cu(2)–N(6)	1.956(7)
O(1W)–Cu(1)–N(1)	98.4(3)	O(1W)–Cu(1)–N(2)	174.7(3)
O(1W)–Cu(1)–N(3)	96.5(3)	O(1W)–Cu(1)–O(2W)	91.6(3)
O(2W)–Cu(1)–N(1)	91.8(3)	O(2W)–Cu(1)–N(2)	93.5(3)
O(2W)–Cu(1)–N(3)	93.0(3)	N(1)–Cu(1)–N(2)	82.5(3)
N(1)–Cu(1)–N(3)	164.2(3)	N(2)–Cu(1)–N(3)	82.2(3)
O(1)–Cu(2)–N(4)	79.4(2)	O(1)–Cu(2)–N(5)	87.3(2)
O(1)–Cu(2)–N(6)	96.6(2)	O(1)–Cu(2)–O(3W)	90.2(3)
O(3W)–Cu(2)–N(4)	96.9(3)	O(3W)–Cu(2)–N(5)	177.5(3)
O(3W)–Cu(2)–N(6)	96.9(3)	N(4)–Cu(2)–N(5)	82.9(3)
N(4)–Cu(2)–N(6)	165.6(3)	N(5)–Cu(2)–N(6)	83.1(3)

Table 3. Interactions of the Cu(II) complexes with CT DNA.[a]

Complex	r[b]	ΔT_m (°C)[c]
1	0.1	0.29
	0.2	0.71
2	0.1	4.22
	0.2	17.8

[a]Reaction conditions: 5 mM pH 7.0 Tris buffer, $I = 0.1$ M NaCl.
[b]r = Molar ratio of complex/nucleic acid phosphate.
[c]ΔT_m (°C) = The melting temperature of DNA with the complex – the melting temperature of free DNA.

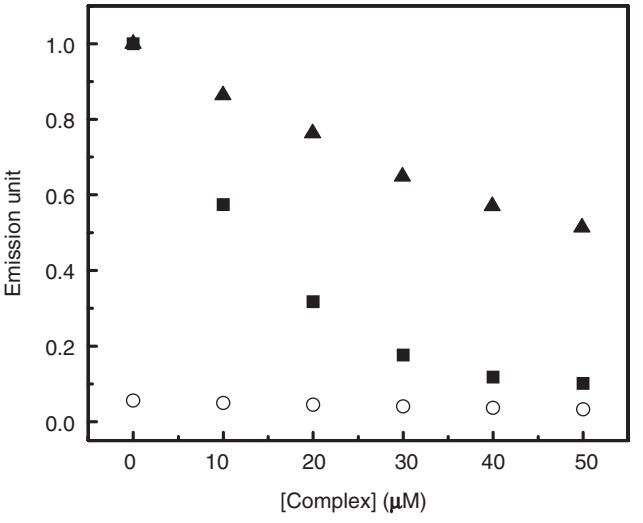

Figure 2. Effects of addition of complexes **1** (▲) and **2** (■) (0–50 μM) on the emission intensity of the CT DNA (285 μM)-bound EB (4.0 μM) in a 5 mM Tris-HCl per 100 mM NaCl buffer (pH 7.0) at room temperature. The emission intensities of EB (in the absence of DNA) at various concentrations of the complex are also shown (o).

Additionally, complexes which interact with DNA by an electrostatic binding mode have no influence on DNA viscosity [53]. The viscosity of DNA decreased sharply with the increase in the concentration of complex **2** (figure 3), indicating that complex **2** partially intercalates between DNA base pairs via its naphthalene ring. On the other hand, the viscosity of DNA was almost unchanged upon the addition of complex **1** (figure 3), suggesting that complex **1** most likely interacts with DNA through an electrostatic interaction.

3.3. *DNA cleavage by the Cu(II) complexes*

The DNA cleavage activities of complexes **1** and **2** were assessed by their abilities to convert the supercoiled pBR322 plasmid DNA (form I) into nicked circular (form II) or linear DNA (form III) in the presence of reducing agents. The DNA cleavages mediated by complexes **1** and **2** exhibited similar time-dependent patterns (figure 4). In both cases, most cleavages were accomplished within 1 min, and longer reaction time did not result in considerable cleavage of extra DNA. However, the cleavage products of complexes **1** and **2** were considerably different. Densitometry analysis showed that the linear DNA (form III) accounted for about 50% of the complex **2** cleavage products, while it contributed only to 10% of the complex **1** cleavage products. This result indicates that complex **2** is more efficient than complex **1** in cleaving double-stranded circular DNA into linear DNA. Based on the structure of complex **2**, the possible existence of an intermediate may explain the cleavage preference of this complex. As shown in Scheme 2, when the naphthalene ring partially intercalates between DNA base pairs, the double-forficiform structure of the cation in complex **2** is adjusted towards both phosphodiester backbones of nucleic acid, thereby facilitating the cleavage of both DNA strands.

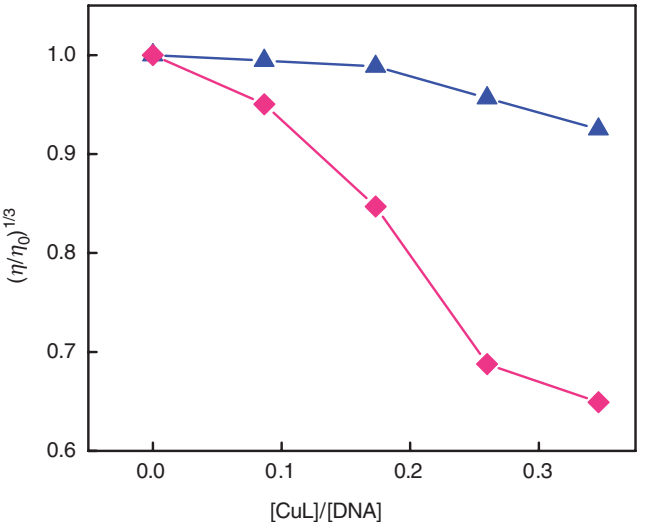

Figure 3. Effects of increasing amounts of complexes **1** (▲) and **2** (■) on the relative viscosities of CT DNA at 30 ± 0.1°C, [DNA] = 0.5 mM, r = [CuL]/[DNA].

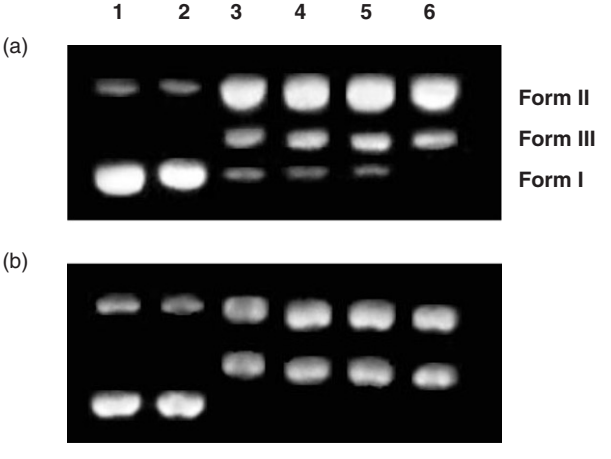

Figure 4. Agarose gel electrophoresis of the DNA cleavage products. Plasmid DNA pBR322 (38 μM) was incubated with 100 μM complexes **1** or **2** in 20 mM HEPES buffer (pH 8.1) at 37°C in the presence or absence of 50 μM H_2O_2 and 50 μM ascorbic acid: (a) Lane 1: DNA control, Lane 2: DNA + **1** (10 min), Lanes 3–6: DNA + **1** + H_2O_2 + ascorbic acid for 1, 2, 5, and 10 min, respectively; (b) Lane 1: DNA control, Lane 2: DNA + **2** (10 min), Lanes 3–6: DNA + **2** + H_2O_2 + ascorbic acid for 1, 2, 5, and 10 min, respectively.

4. Conclusion

Although both synthetic Cu(II) complexes have a naphthalene ring, the dinuclear complex **2** displayed higher DNA affinity and greater DNA cleavage ability than the mononuclear complex **1**. In particular, complex **2** can effectively cleave double-stranded circular DNA into linear DNA. Such cleavage ability may result from the effective cooperation between the naphthalene ring and the base pairs as well as the cooperation

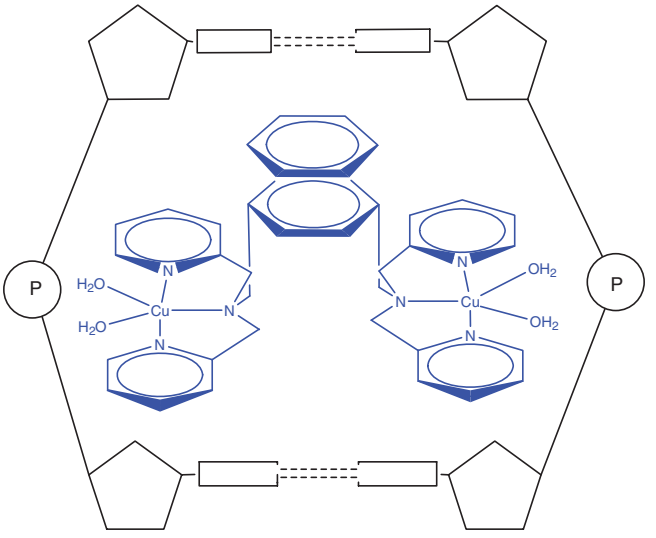

Scheme 2. Proposed interaction mode between complex **2** and DNA.

between the two metal moieties of the dinuclear complex **2** and the phosphodiester backbone of the nucleic acid.

Supplementary material

The ^{1}H NMR and ESI-MS spectra of the ligands and complexes are included as supplementary materials (figures S1 and S2). CCDC 699908 contains the supplementary crystallographic data for the complex **2**. The data can be obtained free of charge via http://www.ccdc.cam.ac.uk/conts/retrieving.html, or from the Cambridge Crystallographic Data Centre, 12 Union Road, Cambridge CB2 1EZ, UK; fax: (+44) 1223-336-033; or Email: deposit@ccdc.cam.ac.uk.

Acknowledgments

This work was supported by the National Natural Science Foundation of China, Guangdong Provincial Natural Science Foundation, and National Basic Research Program of China.

References

[1] Q. Jiang, N. Xiao, P. Shi, Y. Zhu, Z. Guo. *Coord. Chem. Rev.*, **251**, 1951 (2007).
[2] J. Suh. *Acc. Chem. Res.*, **36**, 562 (2003).
[3] A. Sreedhara, J.A. Cowan. *J. Biol. Inorg. Chem.*, **6**, 337 (2001).

[4] N.H. Williams, B. Takasaki, M. Wall. *J. Chin, Acc. Chem. Res.*, **32**, 485 (1999).
[5] E.L. Hegg, J.N. Burstyn. *Coord. Chem. Rev.*, **173**, 133 (1998).
[6] J.A. Cowan. *Chem. Rev.*, **98**, 1067 (1998).
[7] C.J. Burrows, J.G. Muller. *Chem. Rev.*, **98**, 1109 (1998).
[8] W.K. Pogozelski, T.D. Tullius. *Chem. Rev.*, **98**, 1089 (1998).
[9] R.R. Breaker. *Chem. Rev.*, **97**, 371 (1997).
[10] D.E. Wilcox. *Chem. Rev.*, **96**, 2435 (1996).
[11] D.S. Sigman, A. Mazumder, D.M. Perrin. *Chem. Rev.*, **93**, 2295 (1993).
[12] P.A.N. Reddy, M. Nethaji, A.R. Chakravarty. *Eur. J. Inorg. Chem.*, 1440 (2004).
[13] X.M. Xu, J.H. Yao, Z.W. Mao, K.B. Yu, L.N. Ji. *Inorg. Chem. Commun.*, **7**, 803 (2004).
[14] (a) L.P. Lu, M.L. Zhu, P. Yang. *J. Inorg. Biochem.*, **95**, 31 (2003); (b) R. Ren, P. Yang, W.J. Zheng, Z.C. Hua. *Inorg. Chem.*, **39**, 5454 (2000).
[15] A.M. Thomas, M. Nethaji, S. Mahadevan, A.R. Chakravarty. *J. Inorg. Biochem.*, **94**, 171 (2003).
[16] (a) M. Kathryn, T. Deck, A. Tseng, J.N. Burstyn. *Inorg. Chem.*, **41**, 669 (2002); (b) E.L. Hegg, J.N. Burstyn. *Inorg. Chem.*, **35**, 7474 (1996).
[17] J. Gao, A.E. Martell, J. Reibenspies. *Inorg. Chim. Acta*, **329**, 122 (2002).
[18] (a) M. Jezowska-Bojczuk, W. Lesniak, W. Szczepanik, K. Gatner, A. Jezierski, M. Smoluch, W. Bal. *J. Inorg. Biochem.*, **84**, 189 (2001); (b) W. Szczepanik, A. Krezel, M. Brzezowska, E. Dworniczek, M. Jeżowska-Bojczuk. *Inorg. Chim. Acta*, **361**, 2659 (2008).
[19] A. Sreedhara, J.D. Freed, J.A. Cowan. *J. Am. Chem. Soc.*, **122**, 88144 (2000).
[20] (a) D.K. Chand, H.J. Schneider, A. Bencini, A. Bianchi, C. Giorgi, S. Ciattini, B. Valtancoli. *Chem. Eur. J.*, **6**, 400 (2000); (b) D.K. Chand, H.J. Schneider, J.A. Aguilar, F. Escarti, E. Garcia-Espan, S.V. Luis. *Inorg. Chim. Acta*, **316**, 7 (2000).
[21] (a) M.S. Melvin, J.T. Tomlinson, G.R. Saluta, G.L. Kucera, N. Lindquist, R.A. Manderville. *J. Am. Chem. Soc.*, **122**, 6333 (2000); (b) S. Borah, M.S. Melvin, N. Lindquist, R.A. Manderville. *J. Am. Chem. Soc.*, **120**, 4557 (1998).
[22] U. Itoh, H. Hisada, T. Sumiya, M. Hosono, Y. Usui, Y. Fujii. *Chem. Commun.*, 677 (1997).
[23] (a) F.V. Pamatong, C.A. Detmer III, J.R. Bocarsly. *J. Am. Chem. Soc.*, **118**, 5339 (1996); (b) C.A. Detmer III, F.V. Pamatong, J.R. Bocarsly. *Inorg. Chem.*, **35**, 6292 (1996).
[24] Y. Shao, J.Y. Zhang, C. Tu, C.H. Dai, Q. Xu, Z.J. Guo. *J. Inorg. Biochem.*, **99**, 1490 (2005).
[25] S.C. Zhang, Y.G. Zhu, C. Tu, H.Y. Wei, Z. Zhang, L.P. Lin, J. Ding, J.F. Zhang, Z.J. Guo. *J. Inorg. Biochem.*, **98**, 2099 (2004).
[26] Y.M. Zhao, J.H. Zhu, W.J. He, Z. Yang, Y.G. Zhu, Y.Z. Li, J.F. Zhang, Z.J. Guo. *Chem. Eur. J.*, **12**, 6621 (2006).
[27] S.C. Zhang, Y. Shao, C. Tu, C.H. Dai, Z.J. Guo. *Chinese J. Inorg. Chem.*, **20**, 1159 (2004).
[28] M. Gonzalez-Alvarez, G. Alzuet, J. Borras, M. Pitie, B. Meunier. *J. Bio. Inorg. Chem.*, **8**, 644 (2003).
[29] L.P. Lu, M.L. Zhu, P. Yang. *J. Inorg. Biochem.*, **95**, 31 (2003).
[30] D.Y. Kong, J. Reibenspies, J.G. Mao, A. Clearfield, A.E. Martell. *Inorg. Chim. Acta*, **342**, 158 (2003).
[31] L. Zhu, O. dos Santos, C.W. Koo, M. Rybstein, L. Pape, J.W. Canary. *Inorg. Chem.*, **42**, 7912 (2003).
[32] L.M. Rossi, A. Neves, R. Horner, H. Terenzi, B. Szpoganicz, J. Sugai. *Inorg. Chim. Acta*, **337**, 366 (2002).
[33] A.M. Thomas, G. Neelakanta, S. Mahadevan, M. Nethaji, A.R. Chakravarty. *Eur. J. Inorg. Chem.*, 2720 (2002).
[34] (a) K.J. Humphreys, K.D. Karlin, S.E. Rokita. *J. Am. Chem. Soc.*, **124**, 6009 (2002); (b) K.J. Humphreys, A.E. Johnson, K.D. Karlin, S.E. Rokita. *J. Biol. Inorg. Chem.*, **7**, 835 (2002).
[35] G.N. De Iuliis, G.A. Lawrance, S. Fieuw-Makaroff. *Inorg. Chem. Commun.*, **3**, 307 (2000).
[36] C. Tu, Y. Shao, N. Gan, D. Xu, Z.J. Guo. *Inorg. Chem.*, **43**, 4761 (2004).
[37] A. Bencini, E. Berni, A. Bianchi, C. Giorgi, B. Valtancoli, D.K. Chand, H.J. Schneider. *Dalton Trans.*, 793 (2003).
[38] K.J. Humphreys, K.D. Karlin, S.E. Rokita. *J. Am. Chem. Soc.*, **124**, 8055 (2002).
[39] I.O. Fritsky, R. Ott, H. Pritzkow, R. Kramer. *Chem. Eur. J.*, **7**, 1221 (2001).
[40] P. Molenveld, J.F.J. Engbersen, D.N. Reinhoudt. *Angew. Chem. Int. Ed. Engl.*, **38**, 3189 (1999).
[41] S.G. Srivatsan, S. Verma. *Chem. Eur. J.*, **7**, 828 (2001).
[42] (a) J. Suh, S.J. Moon. *Inorg. Chem.*, **40**, 4890 (2001); (b) B.B. Jang, K.P. Lee, D.H. Min, J. Suh. *J. Am. Chem. Soc.*, **120**, 12008 (1998).
[43] R.H. Prince, P.R. Woolley. *Angew. Chem. Int. Ed. Engl.*, **11**, 408 (1972).
[44] M.J. Young, D. Wahnon, R.C. Hynes, J. Chin. *J. Am. Chem. Soc.*, **117**, 9441 (1995).
[45] (a) G.M. Sheldrick. *SHELXS*-97, *Program for Crystal Structure Solution*, Göttingen University, Germany (1997); (b) G.M. Sheldrick. *SHELXL*-97, *Program for Crystal Structure Refinement*, Göttingen University, Germany (1997).
[46] J. Wilson. *International Table for X-ray Crystallography*, Vol. C, Kluwer Academic Publisher, Dordrecht (1992), Tables 4.2.6.8 and 6.1.1.4.

[47] J. He, P. Hu, Y.J. Wang, M.L. Tong, H.Z. Sun, Z.W. Mao, L.N. Ji. *Dalton Trans*., 3207 (2008).
[48] J.B. Chaires, N. Dattagupta, D.M. Crothers. *Biochemistry*, **21**, 3933 (1982).
[49] G. Cohen, H. Eisenberg. *Biopolymers*, **8**, 45 (1969).
[50] S. Satyanarayana, J.C. Dabrowiak, J.B. Chaires. *Biochemistry*, **31**, 9319 (1992).
[51] S. Satyanarayana, J.C. Dabrowiak, J.B. Chaires. *Biochemistry*, **32**, 2573 (1993).
[52] X.H. Zou, B.H. Ye, H. Li, Q.L. Zhang, H. Chao, J.G. Liu, L.N. Ji, X.Y. Li. *J. Biol. Inorg. Chem*., **6**, 143 (2001).
[53] J.G. Liu, B.H. Ye, H. Li, Q.X. Zhen, L.N. Ji, Y.H. Fu. *J. Inorg. Biochem*., **76**, 265 (1999).